The ER Ca^{2+} sensor STIM1 regulates actomyosin contractility of migratory cells

Ying-Ting Chen[1], Yih-Fung Chen[2], Wen-Tai Chiu[1,3], Yang-Kao Wang[4,5], Hsien-Chang Chang[1,5] and Meng-Ru Shen[2,6,7,8,*]

[1]Department of Biomedical Engineering, College of Egineering, National Cheng Kung University, Tainan 701, Taiwan
[2]Department of Pharmacology, College of Medicine, National Cheng Kung University, Tainan 701, Taiwan
[3]Institute of Basic Medical Sciences, College of Medicine, National Cheng Kung University, Tainan 701, Taiwan
[4]Graduate Institute of Biomedical Materials and Tissue Engineering, Taipei Medical University, Taipei 110, Taiwan
[5]Medical Device Innovation Center, National Cheng Kung University, Tainan 701, Taiwan
[6]Department of Obstetrics and Gynecology, National Cheng Kung University Hospital, Tainan 704, Taiwan
[7]Advanced Optoelectronic Technology Center, National Cheng Kung University, Tainan 701, Taiwan
[8]Infectious Diseases and Signaling Research Center, National Cheng Kung University, Tainan 701, Taiwan
*Author for correspondence (mrshen@mail.ncku.edu.tw)

Accepted 21 December 2012
Journal of Cell Science 126, 1260–1267

doi: 10.1242/jcs.121129

Summary

Stromal interaction molecule 1 (STIM1) is an endoplasmic reticulum (ER) Ca^{2+} sensor that triggers the store-operated Ca^{2+} entry (SOCE). The clinical relevance of STIM1 has been highlighted in breast and cervical cancer, but the molecular mechanism by which STIM1 promotes cancer progression remains unclear. This study explores the regulatory mechanisms by which STIM1-dependent Ca^{2+} signaling controls cancer cell migration. Three different SOCE inhibitors, SKF96365, 2-APB and YM-58483, significantly inhibited cervical cancer cell migration to a similar extent to that of STIM1 silencing. In contrast, STIM1 overexpression significantly enhanced cervical cancer cell migration. Live cell confocal images and three-dimensional tomograms showed that STIM1 formed aggregates and translocated towards the plasma membranes of migratory cells, and this was accompanied by increasing cytosolic Ca^{2+} spikes. STIM1 silencing also inhibited the recruitment and association of active focal adhesion kinase (pTyr397-FAK) and talin at focal adhesions, indicating the blockade of force transduction from integrin signaling. Epidermal growth factor-induced phosphorylation of myosin II regulatory light chains was abolished by STIM1 knockdown and SOCE inhibition. Dual immunostaining of activated myosin II (pSer19-MLC) and actin revealed that actomyosin formation depended on STIM1-mediated Ca^{2+} entry. Most importantly, STIM1 expression levels as well as SOCE activity controlled the generation of cell contractile force, as measured by the microfabricated post-array-detector system. These results highlight the unique role of STIM1-dependent Ca^{2+} signaling in controlling cell migration by the regulation of actomyosin reorganization in conjunction with enhanced contractile forces.

Key words: Stromal-interaction molecule 1, Actomyosin, Contractile force, Microfabricated post-array detectors

Introduction

Cell migration is an essential process during embryonic development, wound healing, angiogenesis and immunological chemotaxis. The cycling of multi-step processes is involved in cell migration, such as front edge extension, new adhesion formation, cytoskeletal contraction, and rear end detachment (Ridley, 2011). Cell migration is also an early requirement for cancer metastasis when cancer cells acquire invasive behavior and disseminate through the nearby blood and lymph vessels (Mierke et al., 2008; Yang et al., 2009; Yilmaz and Christofori, 2009). Migratory cells exert contractile force to supply the rear-end retraction and forward protrusion (Ananthakrishnan and Ehrlicher, 2007). While these contractile forces are important for the regulation of focal adhesion turnover and cytoskeletal organization in cell migration, the mechanisms that control force generation during cell migration are not well understood.

Modulation of cytosolic Ca^{2+} levels provides versatile and dynamic signaling involved in various cellular processes, such as proliferation, migration and gene regulation (Berridge et al., 2003). Store-operated Ca^{2+} entry (SOCE) is a major Ca^{2+} entry pathway in nonexcitable cells (Parekh, 2010; Putney, 2005). SOCE, by definition, is activated by Ca^{2+} release from the internal store. The activation of SOCE includes several steps. (1) Stimulation of G proteins or protein tyrosine kinases activates phospholipase C (PLC), which hydrolyzes phosphatidylinositol bisphosphate to release the second messenger inositol 1,4,5-trisphosphate. (2) Binding of inositol 1,4,5-trisphosphate to its receptor in the endoplasmic reticulum (ER) membrane causes rapid and transient Ca^{2+} release from the ER lumen. (3) The decrease of ER luminal Ca^{2+} activates store-operated Ca^{2+} (SOC) channels in the plasma membrane, leading to a sustained influx of extracellular Ca^{2+} across the plasma membrane (reviewed in Parekh, 2010; Várnai et al., 2009). Two genes, *STIM1* (stromal-interaction molecule 1) and *Orai1*, are responsible for SOCE activation (Parekh, 2010). The STIM1 molecule functions as an ER Ca^{2+} sensor that detects store depletion. Once ER Ca^{2+} is depleted, STIM1 proteins form many aggregates and translocate close to the plasma membrane. Orai1, an essential pore-forming component of the SOC channel, translocates to the same

STIM1-containing structures during store depletion and opens to mediate Ca^{2+} entry.

The physiological importance of STIM1 has mostly been studied in immune systems. STIM1 is required for the development and function of regulatory T cells (Oh-Hora et al., 2008; Qu et al., 2011) and STIM1 deficiency causes several autoimmune diseases and myopathy in human subjects and mouse models (Feske, 2009). The emerging importance of STIM1 in tumor biology has been highlighted in breast and cervical cancer (Chen et al., 2011; Yang et al., 2009). Inhibiting STIM1-mediated Ca^{2+} influx impairs the focal adhesion turnover of breast cancer cells, which can be rescued by the small GTPases Ras and Rac (Yang et al., 2009). In addition, reduction of Orai1 or STIM1 by RNA interference in highly metastatic human breast cancer cells, or treatment with a pharmacological inhibitor of SOCE, decreases tumor metastasis in animal models. Our previous study further demonstrated that STIM1 is a key regulator for the epidermal growth factor (EGF)-induced Ca^{2+} influx that is necessary for the activation of Ca^{2+}-dependent protease calpain and tyrosine kinase Pyk2 (Chen et al., 2011). More importantly, our findings from analyzing surgical specimens suggested that the pathological significance of tumor STIM1 overexpression is that it increases the locomotion of cancer cells.

The efficiency of cell migration is regulated by the dynamic interactions between the cytoskeleton, non-muscle myosin II and focal adhesions (Kadir et al., 2011). The association between actin filaments and myosin II forms contractile actomyosin fibers that regulate various biological processes, including cytokinesis, adhesion and migration (Sanz-Moreno et al., 2011). Although our and other studies have demonstrated that STIM1-dependent signaling regulates focal adhesion turnover and cell migration (Chen et al., 2011; Yang et al., 2009), an important remaining question is whether STIM1-dependent signaling integrates the dynamic interactions between actomyosin and focal adhesions to mediate efficient cell migration. In the current study we demonstrated that STIM1 expression and SOCE activity are necessary for cell migration through the regulation of actomyosin reorganization in conjunction with enhanced contractile forces.

Results

Cancer cell migration depends on STIM1 expression and SOCE activity

We established several stable pools of SiHa cervical cancer cells with different levels of STIM1 expression to study its role in cell migration (Fig. 1A). Transfection with STIM1-specific shRNAs optimally reduced STIM1 protein levels. In the presence of STIM1-specific shRNAs, the migration of SiHa cells was reduced by 40–50% (Fig. 1B). In contrast, STIM1 overexpression significantly enhanced cervical cancer cell migration. We also studied whether the blockade of SOCE activity alters cervical cancer cell migration. SKF96365 and 2-APB are potent inhibitors of SOCE in cervical cancer cells (Chen et al., 2011). YM-58483 also inhibited SOCE of cervical cancer cells in a dose-dependent manner (supplementary material Fig. S1). SKF96365 significantly inhibited cervical cancer cell migration to a similar extent by STIM1 silencing (Fig. 1B). Moreover, both 2-APB and YM-58483 dose-dependently inhibited cervical cancer cell migration. These

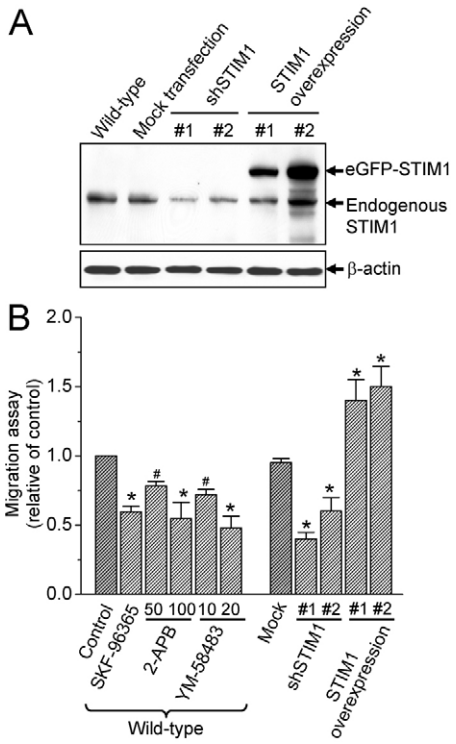

Fig. 1. STIM1 expression and SOCE activity are involved in cervical cancer cell migration. (**A**) The different levels of STIM1 expression in several stable pools of SiHa cervical cancer cells. (**B**) Migration of cells after treatment as indicated. STIM1 expression levels and SOCE activity affect cervical cancer cell migration. Values are means ± s.e.m. from at least three different experiments. SOCE inhibitors: SKF96365 (50 μM), 2-APB (50 and 100 μM) and YM-58483 (10 and 20 μM). $^{\#}P<0.05$, $^{*}P<0.01$, compared with control group.

results indicate that STIM1 expression levels, as well as SOCE activity, are associated with cervical cancer cell migration.

The polarized distribution of intracellular Ca^{2+} is known to be involved in the regulation of cell migration (Wei et al., 2009). We previously showed that STIM1-dependent Ca^{2+} signaling played an important role in EGF-stimulated cancer cell migration (Chen et al., 2011). EGF stimulates the aggregation and translocation of STIM1 towards to the Orai1-containing regions of the plasma membrane to mediate SOCE (Chen et al., 2011). It is thus of interest to monitor the spatial and temporal distribution of cytosolic Ca^{2+} spikes and STIM1 in migratory cells. We performed time-lapse confocal image recordings of cervical cancer cells upon EGF stimulation (supplementary material Movie 1). As shown in Fig. 2A,B, STIM1 was scattered in the cytosol prior to EGF stimulation. EGF induced STIM1 aggregation into many clusters that localized to regions near or at the plasma membrane, especially at both polar ends of migratory cells. The translocation of STIM1 clusters became obvious 5–10 minutes after EGF stimulation. The three-dimensional (3D) tomograms also indicated that EGF stimulated the formation of STIM1 aggregates that translocated towards the plasma membrane (Fig. 2C; supplementary material Movies 3, 4). Moreover, the STIM1 aggregation was accompanied by increased cytosolic Ca^{2+} spikes, as visualized by the Ca^{2+}-sensitive fluorescent dye Fluo-4 (Fig. 3A,B; supplementary material Movie 4).

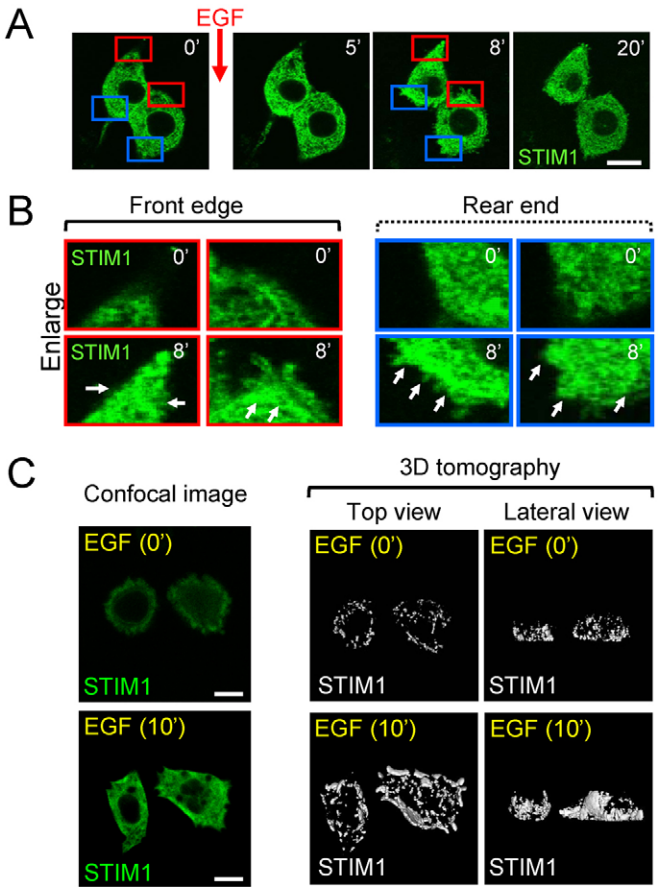

Fig. 2. STIM1 forms aggregates and translocates towards plasma membranes in migratory cells. (**A**) Time-lapse confocal images from supplementary material Movie 1, of SiHa cells after stimulation with 100 ng/ml EGF. EGF induced aggregation of STIM1 into many clusters that moved towards the plasma membrane of both polar ends in migratory cells. Scale bar: 10 µm. (**B**) Enlarged views of the areas indicated by colored rectangles in whole cell images in A. Arrows indicate EGFP–STIM1 aggregation. (**C**) Localization of EGF-stimulated STIM1 cluster formation near or at the plasma membrane. Left: expression of EGFP–STIM1 after treatment with 100 ng/ml EGF. Right: 3D tomograms of STIM1 aggregates, adapted from supplementary material Movies 2 and 3. Scale bars: 10 µm.

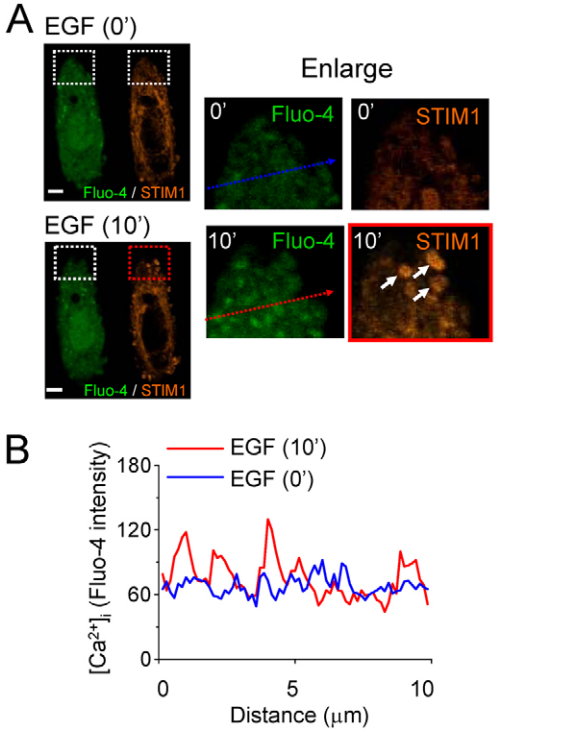

Fig. 3. EGF-stimulated STIM1 aggregate formation is accompanied by increased cytosolic Ca^{2+} spikes. Cytosolic Ca^{2+} distribution was estimated using the fluorescent Ca^{2+} indicator Fluo-4/AM in SiHa cells expressing mOrange–STIM1. (**A**) Left: whole cell images. Right: the enlargements of areas indicated by the colored rectangles in the whole cell images. Arrows indicate the aggregation of mOrange–STIM1. Dashed line, the area for (**B**) Quantitative analyses of Fluo-4 fluorescence intensity shown along the dotted lines in A. These images were adapted from supplementary material Movie 2. Scale bars: 10 µm.

STIM1-dependent Ca^{2+} signaling regulates actomyosin formation

Migratory cells generate intracellular forces that act on the surrounding extracellular matrix or neighboring cells (Milner and Campbell, 2002). This contractile activity is crucial for a number of signal transductions that regulate cell migration. The contractile forces of migratory cells are regulated by dynamic focal adhesions and also controlled by actomyosin contractility. The interaction between focal adhesion kinase (FAK) and talin is required for focal adhesion turnover and cell motility (Lawson et al., 2012). FAK is a cytoplasmic tyrosine kinase that phosphorylates targets such as paxillin to regulate adhesion dynamics. Talin is a large cytoskeletal protein that binds integrin cytoplasmic tails and FAK, and plays a key role in integrin-mediated force transduction and cell migration. We studied the effect of STIM1 expression on the force transduction of focal adhesions by double-staining of pTyr397-FAK and talin, which represents the functional layers of integrin signaling and force transduction (Kanchanawong et al., 2010). As shown in Fig. 4, EGF induced the recruitment of active FAK (pTyr397-FAK) to focal adhesions, where pTyr397-FAK was associated with variably sized, diagonally oriented arrays of talin. In contrast, STIM1 knockdown abolished EGF-induced recruitment and association of pTyr397-FAK and talin at focal adhesions, indicating that STIM1 expression is necessary for the force transduction of the focal adhesion network.

Non-muscle cell contractility is controlled by non-muscle myosin II, through the phosphorylation of its regulatory light chains (MLC2) in a Ca^{2+}/calmodulin-dependent manner (Vicente-Manzanares et al., 2009). We studied whether STIM1-dependent Ca^{2+} signaling and SOCE activity are involved in the regulation of MLC2 activation. As shown in Fig. 5A, EGF significantly increased the phosphorylation levels of MLC2 at Ser19 (pSer19-MLC) that had been almost abolished by SKF96365, a SOCE inhibitor in cervical cancer cells (Chen et al., 2011). STIM1 knockdown by siRNA also significantly attenuated EGF-induced MLC2 phosphorylation at Ser19 (Fig. 5B). These results indicate that STIM1-dependent Ca^{2+} signaling have a great impact on MLC2 activation.

We further studied the association between EGF stimulation, STIM1 abundance and actomyosin contractility. Actomyosin is a complex of actin filaments and non-muscle myosin II. To study the expression of actomyosin, SiHa cells were

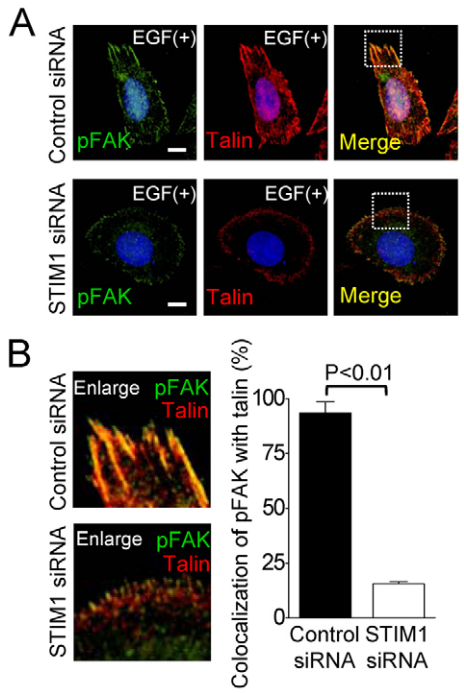

Fig. 4. STIM1 modulates the association between talin and active FAK at focal adhesions. (**A**) Representative confocal images showing the association between talin (red) and phospho-FAK (Tyr397; green) at focal adhesions. Nuclei were stained with Hoechst 33258 (blue). Scale bars: 10 μm. (**B**) Left panel: enlargements of the areas indicated by the color rectangles in A. Right panel: colocalization ratio between talin and phospho-FAK (Tyr397) at focal adhesions, quantified by pixel-by-pixel analyses. pFAK, phospho-FAK (Tyr397). Values are means ± s.e.m. from at least 25 individual cells.

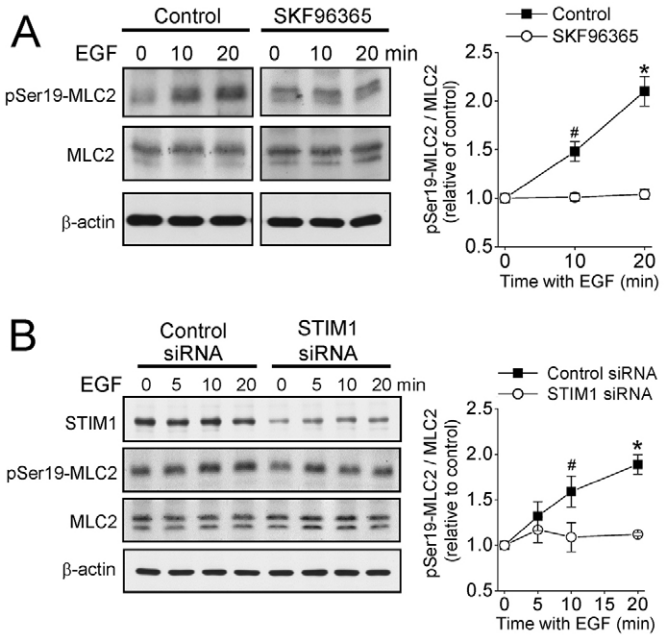

Fig. 5. SOCE and STIM1 are involved in the regulation of non-muscle myosin II activation. (**A**,**B**) EGF induces phosphorylation of myosin II regulatory light chains that are inhibited by the SOCE inhibitor SKF96365 (50 μM; A) or STIM1 knockdown (B). Left panels: representative immunoblots from four different experiments showing the phosphorylation (Ser19) of myosin II regulatory light chains (MLC2). Right panels: densitometric quantification of MLC2 phosphorylation levels. Values are means ± s.e.m. $^{\#}P<0.05$, $^{*}P<0.01$, compared with control groups.

double-immunostained with activated myosin II (pSer19-MLC) and actin. As shown in Fig. 6A, the quiescent cells had well-organized cortical actin cytoskeletons at the cell periphery, and the intensity of pSer19-MLC fluorescence was scanty. EGF stimulation induced the reorganization of actin stress fibers at cell protrusions, where pSer19-MLC aligned along the actin filaments, indicating the increased expression of actomyosin (Fig. 6A). STIM1 knockdown by siRNA almost abolished EGF-induced actomyosin formation compared with control siRNA treatment (Fig. 6B). In contrast, STIM1 overexpression significantly enhanced actomyosin expression in response to EGF stimulation, compared to that of mock transfection (Fig. 6C,D). As summarized in Fig. 6E, EGF-induced reorganization of actomyosin in cervical cancer cells depends on STIM1 abundance. The role of Ca^{2+} entry in regulating actomyosin formation was also studied. Blocking Ca^{2+} influx by removal of external Ca^{2+} almost abolished EGF-stimulated actomyosin formation (Fig. 7A,B). In addition, results from three different SOCE inhibitors demonstrated that SOCE activity is involved in the regulation of actomyosin reorganization (Fig. 7C,D). Taken together, these results indicated that STIM1-mediated SOCE is an important pathway controlling actomyosin reorganization.

SOCE and STIM1 are involved in the regulation of contractile force

Cell migration involves dynamic adhesive processes and cytoskeleton remodeling, leading to contraction between cells and the surrounding extracellular matrix. The current study and our previous results (Chen et al., 2011) show that STIM1 was crucially involved in EGF-induced focal adhesion turnover and actomyosin reorganization. To reveal the important role of STIM1 in the regulation of cell contraction, the microfabricated post-array-detector (mPAD) system was used to measure cell contractile force at a single adhesion site (Fu et al., 2010; Tan et al., 2003). The micropillars of mPAD were 3 μm in diameter, 8 μm tall, and were configured in a regular array with 9 μm center-to-center spacing (supplementary material Fig. S2). We stained the mPAD with 1,1′-dioctadecyl-3,3,3′3′-tetramethylindocarbocyanine perchlorate (DiI), a hydrophobic and lipophilic cyanine dye, for visualization with confocal microscopy. The top of the pillar was coated with fibronectin to assist cell adhesion. SiHa cells were cultured on mPADs and the whole system was scanned using confocal microscopy (Fig. 8A; supplementary material Movie 5). Cells generated contractile force pulling on the adherent micropillars (Fig. 8B). The contractile force (F) on the micropillars was calculated by the displacement (ΔX) and spring constant of the micropillars (Fig. 8C). The displacement of micropillars was measured as the deviation of the top of the pillar with reference to the bottom (Fig. 8D, top and bottom of the micropillar are colored grey and red, respectively). This method thus provides a quantitative and temporal definition of the nanonewton (nN)-ranged traction force between the cells and the extracellular matrix at the micropillars (Fu et al., 2010; Tan et al., 2003).

SiHa cells were cultured on the mPAD system under various experimental conditions to evaluate the effect of STIM1 expression and SOCE activity on cell contractility. Fig. 8D showed the real-time measurements of traction force at single

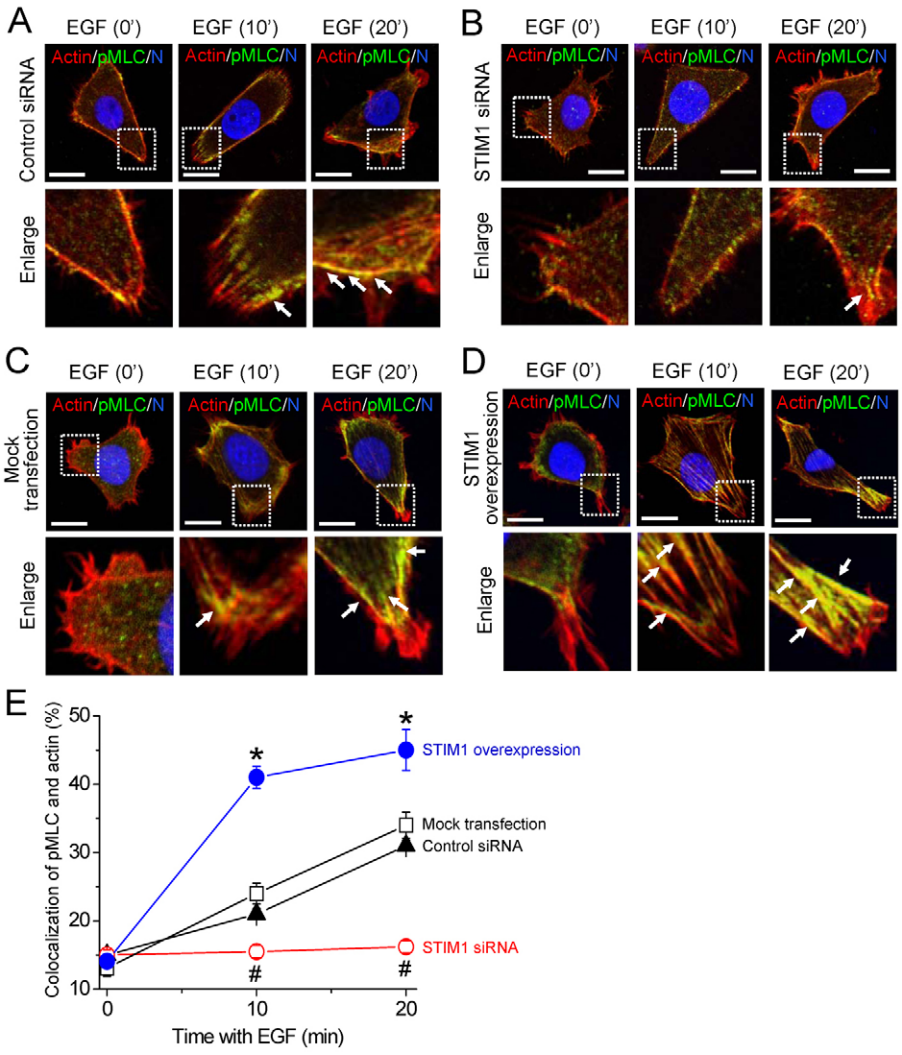

Fig. 6. The formation of actomyosin depends on STIM1 expression levels. (**A**,**B**) EGF induces the formation of actomyosin that is significantly inhibited by STIM1 silencing. Representative confocal images showing the expression of phosphorylated MLC2 (pMLC; green) and F-actin (red) at the cell periphery. Nuclei were stained with Hoechst 33258 (blue). Scale bars: 10 µm. Arrows indicate actomyosin formation as indicated by the association of phospho-MLC2 (Ser19) and F-actin. pMLC, phospho-MLC2 (Ser19). (**C**,**D**) STIM1 overexpression significantly enhanced EGF-induced actomyosin expression. The lower row of images in each panel show enlargements of the areas indicated by colored rectangles in the whole cell images. (**E**) Quantitative pixel-by-pixel analyses of colocalization between phospho-MLC2 (Ser19) and F-actin. Values are means ± s.e.m. from at least 15 individual cells. $^{\#}P<0.05$, $^{*}P<0.01$, compared with control groups.

micropillar generated by STIM1-overexpressing SiHa cells in response to EGF stimulation. The cell contractile force is defined as the sum of the traction force applied at each micropillar (Fig. 8E). Compared with mock-transfected cells, STIM1 overexpression significantly enhanced the amplitude of the contractile force (Fig. 8E). More importantly, both the SOCE inhibitor SKF96365 and the intracellular Ca^{2+} chelator BAPTA-AM abolished EGF-induced contractile force generation (Fig. 8E). These results indicate that STIM1-dependent Ca^{2+} signaling and SOCE activation induce actomyosin reorganization in conjunction with enhanced contractile forces.

Discussion

This study highlights the important role of STIM1-dependent Ca^{2+} signaling in controlling cell migration. STIM1 expression levels as well as SOCE activation are functionally linked with cell migration through the regulation of actomyosin reorganization in conjunction with enhanced contractile forces. This conclusion is supported by the following evidence. (1) STIM1 overexpression enhanced cervical cancer cell migration, whereas RNA interference targeting STIM1 suppressed it. Blocking SOCE by the use of inhibitors decreased cervical cancer cell migration to a similar extent as that seen with STIM1 knockdown, suggesting that STIM1-dependent SOCE plays an important role in cervical cancer cell migration. (2) STIM1 knockdown inhibited the recruitment and association of pTyr397-FAK and talin at focal adhesions, indicating the blockade of force transduction from integrin signaling. (3) MLC2 phosphorylation was closely associated with STIM1 expression as well as SOCE activity. Consistent with this, actomyosin formation in migratory cells depended on STIM1-mediated Ca^{2+} entry. (4) The direct measurement of cell contractility confirmed that the generation of cell contractile force required STIM1-dependent SOCE.

In this study, we demonstrated that STIM1-mediated SOCE plays an important role in regulating cervical cancer cell migration. Interestingly, both STIM1 knockdown with two different shRNA duplexes and SOCE blockade with three different potent inhibitors significantly reduced cervical cancer cell migration by 50% (Fig. 1B), indicating that other Ca^{2+} entry pathways contributed to cervical cancer cell migration. Several plasmalemmal Ca^{2+} channels have been suggested as important in regulating cancer cell migration (reviewed in Prevarskaya et al., 2011; Monteith et al., 2012). For example, the Ca^{2+}-permeable transient receptor potential (TRP) channel family has been implicated in migration of various cancer cell types. A pro-migratory role of TRPM7 was demonstrated in breast cancer

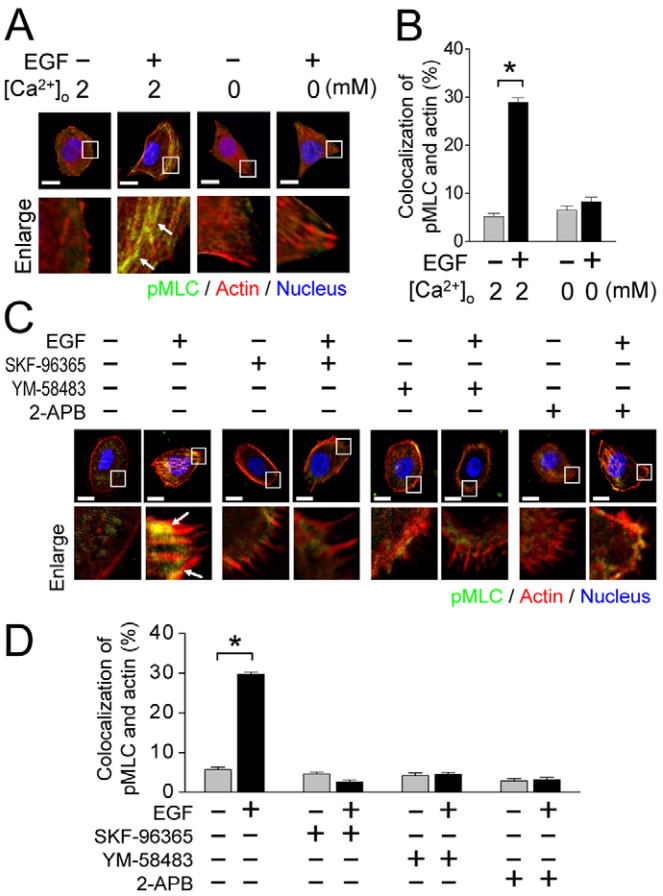

Fig. 7. Extracellular Ca^{2+} and SOCE activity are important in the regulation of actomyosin formation. (**A**,**B**) Effect of extracellular Ca^{2+} on actomyosin formation. SiHa cells were treated with Ca^{2+}-free medium to prevent Ca^{2+} entry. (**C**,**D**) EGF induces the formation of actomyosin, which is significantly inhibited by SOCE inhibitors. Cells were pre-incubated with 0.1% DMSO or SKF96365 (50 µM), 2-APB (100 µM) and YM-58483 (10 µM) for 1 hour prior to EGF (100 ng/ml, 20 minutes) stimulation. (A,C) Representative confocal images showing the expression of phosphorylated MLC2 (pMLC) and F-actin. Nuclei were stained with Hoechst 33258 (blue). Scale bars: 10 µm. (B,D) Quantitative pixel-by-pixel analyses of colocalization between phospho-MLC2 (Ser19) and F-actin. Values are means ± s.e.m. from at least 15 individual cells. *P<0.01, compared with control groups.

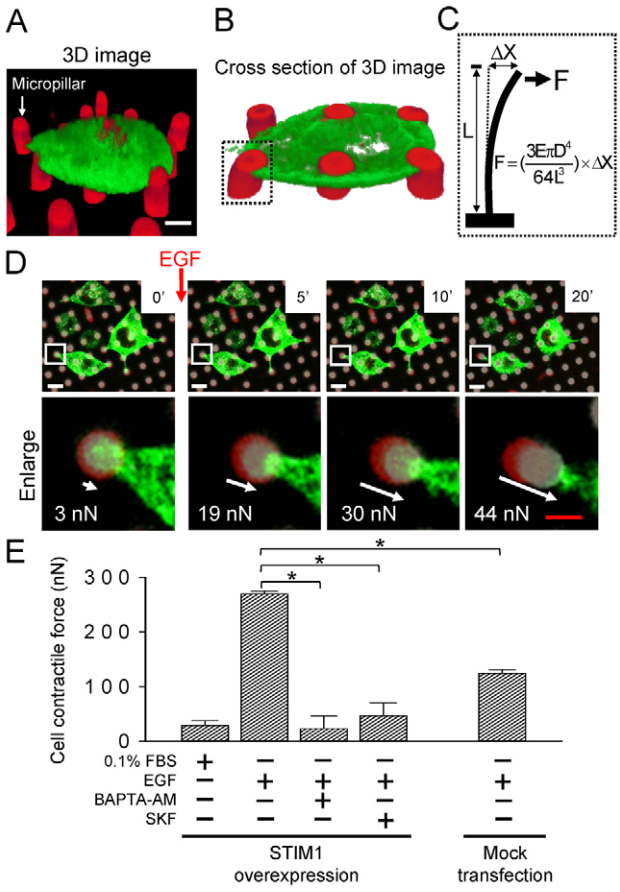

Fig. 8. STIM1-mediated Ca^{2+} signaling regulates the cellular contractile force. (**A**) 3D image of SiHa cells cultured on an mPAD (adapted from supplementary material Movie 3). (**B**) Cross section of a 3D image of the top of a micropillar showing that a cell contracts and pulls the adherent micropillar. (**C**) The contractile forces (F) on a single adhesion site were calculated using the displacement (ΔX) and spring constant of a micropillar; E, Young's modulus; D, diameter; L, length and ΔX, deflection of the micropillar. (**D**) Top: the real-time images of contractile force generation for STIM1-overexpressing SiHa cells cultured on mPADs. Lower: quantitative and temporal definition of the nanonewton (nN)-ranged contractile force between cells and extracellular matrix at single focal adhesion site. The top and bottom of the micropillar are colored grey and red, respectively. Scale bars: 10 µm. (**E**) Ca^{2+} influx and STIM1 are involved in the regulation of cellular traction force. SiHa cells with different expression levels of STIM1 were cultured on the mPAD system. The SOCE inhibitor SKF96365 (50 µM) or cytosolic Ca^{2+} chelator BAPTA-AM (20 µM) was added 10 min prior to EGF stimulation (100 ng/ml, 15 min). Values are means ± s.e.m. from at least 15 different cells.

cells, in which TRPM7 silencing interfered with focal adhesion dynamics and significantly decreased cellular migratory potential (Middelbeek et al., 2012). In prostate cancer cells, it has been shown that the expression of TRPV2 was correlated with cell migration through the induction of the invasive enzymes matrix metalloproteinase (MMP)-2, MMP-9 and cathepsin B (Monet et al., 2010). It thus remains possible that SOCE activity is an important pathway, but not the only one, controlling cervical cancer cell migration.

Our results showed the unique role of STIM1 in controlling the mechanotransduction of migratory cells. Migratory cells can generate intracellular forces that act on the surrounding extracellular matrix or neighboring cells, and this contractile activity is important for several signal transductions essential for cell migration. Non-muscle myosin II is the major motor protein driving cellular contractility. The bipolar filaments of myosin II pull together antiparallel oriented actin filaments to generate cortical tension. The phosphorylation of regulatory light chains by Ca^{2+}-dependent MLC kinase (MLCK) is the major regulator for the myosin-II-based contractile responses. Myosin-II-based actomyosin contraction is transmitted to focal adhesions to establish contractile force that relocates the cell body and contributes to cell movement. The importance of STIM1-dependent Ca^{2+} signaling in focal adhesion turnover during cancer cell migration has been demonstrated in previous studies (Chen et al., 2011; Yang et al., 2009). By the direct measurement of cell traction forces, our results showed for the first time that STIM1-dependent Ca^{2+} signaling regulated the traction force generation at focal adhesions. The influence of STIM1 abundance

on contractile force generation was consistent with that on actomyosin reorganization, as visualized by immunostaining of activated myosin II molecules and actin stress fibers.

Taken together with our previous study (Chen et al., 2011), we propose the following mechanisms by which STIM1-dependent Ca^{2+} signaling regulates cell force transmission during migration. One involves integrin signaling, which regulates the recruitment of Pyk2, FAK and talin to focal adhesions, and the other controls the formation of actomyosin by regulating phosphorylation of the myosin II regulatory light chain. In conclusion, the interaction between STIM1 and the plasma membrane SOC channel Orai1 activates the Ca^{2+} influx that induces actomyosin reorganization in conjunction with enhanced contractile forces (summarized in supplementary material Fig. S3). This study suggests that blocking STIM1-mediated Ca^{2+} signaling is a potential approach to inhibit cancer cell migration.

Materials and Methods

Cell culture and transfection

Cultures of SiHa human cervical cancer cells were prepared as previously described (Chen et al., 2011; Chiu et al., 2008). Ca^{2+}-free Dulbecco's modified Eagle's medium (DMEM) was purchased from Invitrogen. Stable pools of cervical cancer cells overexpressing human STIM1 were used in this study. The full-length cDNA of EGFP-STIM1 and mOrange-STIM1 were kindly provided by Liangyi Chen of the Chinese Academy of Science, China (Xu et al., 2006). EGFP- or mOrange-STIM1 cDNA plasmids were transfected into SiHa cells using Lipofectamine 2000 (Invitrogen) and cells with STIM1 overexpression were selected by G418 (Sigma-Aldrich). A FACSAria cell sorter (BD Biosciences) was used to isolate the stable pools of cells overexpressing human STIM1.

RNA interference

The details of RNAi targeting and preparation were described previously (Chen et al., 2011). For small interfering RNA (siRNA)-mediated knockdown of STIM1, cells were transfected with 100 nM of either the targeting or control siRNA (Santa Cruz Biotechnology) using Lipofectamine 2000 (Invitrogen) for 48 hours. The functional assays were subsequently carried out after validation of STIM1 knockdown without affecting the cell viability. Several independent duplexes of siRNAs (synthesized by Invitrogen) and the siRNA pools of three duplexes (Santa Cruz Biotechnology) were used to target each gene. The sequences of siRNA targeting human STIM1 are as follows: (i) sense, 5′-UUGAGAGGAAACUUCUUCCGGCCUGtt-3′; antisense, 5′-CAGGCCGGAAGAAGUUUCCUCUCAAtt-3′; (ii) sense, 5′-UAACGGUUCUGGAUAUAGGCAAACCtt-3′; antisense, 5′-GGUUUGCCUAUAUCCAGAACCGUUAtt-3′; (iii) the STIM1 siRNA pool of three duplexes: sense, 5′-CUGGUGGUGUCUAUCGUUAtt-3′; antisense, 5′-UAACGAUAGACACCACCAGtt-3′; sense, 5′-CCACUUCAGUGCAUGUCUUtt-3′; antisense, 5′-AAGACAUGCACUGAAGUGGtt-3′; sense, 5′-CAGGAGGAUUUGUCUCUAAtt-3′; antisense, 5′-UUAGAGACAAAUCCUCCUGtt-3′. To establish stable pools of SiHa cells with STIM1 knockdown, two different pools of short hairpin RNAs (shRNAs) targeting human STIM1 (from Santa Cruz Biotechnology and OriGene) or control shRNA (Santa Cruz Biotechnology) were introduced into SiHa cells by electroporation (MicroPorator-mini MP-100, Digital Bio Technology), and selected using 350 ng/ml puromycin (Sigma-Aldrich). The sequences of shRNA pools targeting human STIM1 are as follows: (i) 5′-CTGGTGGTGTCTATCGTTATTCAAGAGATAACGATAGACACCACCAGTTT-3′; 5′-CAGGAGGATTTGTCTCTAATTCAAGAGATTAGAGACAAATCCTCTGTTTTT-3′ (Santa Cruz Biotechnology). (ii) 5′-GATGATGCCAATGGTGATGTGGGATGTGGA-3′; 5′-ACAGTGAAACATAGCACCTTCCATGGTGA-3′; 5′-CTGCTGGTTTGCCTATATCCAGAACCGTT-3′; 5′-CTGAGCAGAGTCTGCATGACCTTCAGGAA-3′ (OriGene).

Primary antibodies and reagents

The antibody against STIM1 (clone 44) was from BD Biosciences. The antibody against β-actin (clone AC-15) was from Sigma-Aldrich. The antibody against phospho-Tyr397-FAK (catalog number 44-624G) was from Invitrogen. Antibodies against myosin-light cahin-2 (MLC-2; catalog number 3672) and phospho-Ser19-MLC (pMLC; catalog number 3671) were from Cell Signaling. The antibody against talin (clone TD77) was from Millipore. EGF and YM-58483 were from Sigma-Aldrich. SKF96365 and 2-APB were from Cayman Chemical. 1,2-*bis*(*o*-aminophenoxy)ethane-*N,N,N′,N′*-tetraacetic acid tetra(acetoxymethyl) ester (BAPTA-AM) was from Merck-Millipore. Fluo-4/AM was from Invitrogen.

Immunoblotting

For immunoblotting, cells were harvested with ice-cold modified radioimmune precipitation assay (RIPA) buffer containing a protease inhibitor cocktail (Roche Diagnostics), 100 mM KCl, 80 mM NaF, 10 mM EGTA, 50 mM h-glycerophosphate, 10 mM p-nitrophenyl phosphate, 1 mM vanadate, 0.5% sodium deoxycholate, and 1% NP40. Protein concentrations were determined with the use of a Bio-Rad protein assay. Equal amounts of protein lysates were separated by SDS-PAGE, and then transferred to nitrocellulose blotting membranes (Pall). Immunoblots were blocked, incubated with the primary antibody, washed, and incubated with the corresponding horseradish-peroxidase-conjugated secondary antibody (Jackson ImmunoResearch), and visualized by western blotting luminol reagent (Santa Cruz Biotechnology). Bands in the immunoblots were quantified using Vision WorksLS software (UVP).

Migration assay

For cell migration assay, cells were allowed to migrate across a Transwell (with 8 μm pore membranes; Corning Incorporated) towards the medium containing 10 μg/ml fibronectin for 12 hours at 37℃. Cells that migrated through the membrane were then fixed with methanol, stained with GIEMSA stain, and counted immediately.

Immunofluorescence, confocal microscopy and image analyses

For immunofluorescent staining, cells were seeded on glass coverslips. Cells were fixed with 4% paraformaldehyde, permeabilized with 0.1% Triton X-100 for 15 min, and blocked with commercial blocking serum (Invitrogen). The cells were incubated with primary antibody at 4℃ overnight, washed, and then incubated with Alexa-Fluor-conjugated secondary antibodies (Invitrogen) for 1 hour at room temperature. To detect nuclei and actin filaments, cells were stained with Hoechst 33258 and phalloidin conjugated with tetramethylrhodamine B isothiocyanate (TRITC; Sigma-Aldrich) for 1 hour at room temperature. The cells were then washed and mounted, and the fluorophores were excited by a laser at 405, 488, or 543 nm and examined with a scanning confocal microscope (FV-1000, Olympus). For the live-cell imaging, cells overexpressing EGFP–STIM1 were directly activated by a laser at 488 nm for the detection of EGFP. The fluorescent Ca^{2+} indicator Fluo4/AM (Invitrogen) was used to estimate cytosolic Ca^{2+} levels. The colocalization of different molecules in confocal images was assessed using pixel-by-pixel analysis and FV-1000 software. The 3D images of mPADs and the 3D tomography of STIM1 were reconstructed from serial confocal Z-section scanning images using Avizo 3D imaging and analysis software (Version 6.0, Mercury computer systems).

Preparation of the mPAD system and measurement of contractile forces

The fabrication of the microfabricated post-array-detector (mPAD) system and contractile force measurement were performed as previously described (Fu et al., 2010; Tan et al., 2003), following the procedure illustrated in the supplementary material Fig. S3. The contractile force on each adhesion site was calculated using Hooke's Law and the displacement and spring constant of the micropillars (Fig. 8C). The displacement was measured as the deviation of the top (deflected position) from the bottom (un-deflected position) of the micropillar from serial confocal Z-section scanning images.

Statistics

All values are reported as means ± s.e.m. (standard error of the mean). Student's paired or unpaired *t*-tests were used for statistical analyses. Differences between values were considered significant when $P<0.05$.

Acknowledgements

We thank Dr Liangyi Chen at the Chinese Academy of Science for STIM1 plasmids.

Author contributions

Y.T.C., Y.F.C., W.T.C., Y.K.W., H.C.C., and M.R.S. designed research; Y.T.C., Y.F.C., W.T.C., and Y.K.W. performed research; Y.T.C., Y.F.C., W.T.C., Y.K.W., and M.R.S. analyzed data; and Y.T.C., Y.F.C., and M.R.S. wrote the article.

Funding

This work was partly supported by National Science Council [NSC 101-2321-B-006-019 to M.R.S.], National Health Research Institutes [NHRI-EX102-10243BI to M.R.S.], Department of Health, Executive Yuan and National Cheng Kung University Hospital, Taiwan.

Supplementary material available online at
http://jcs.biologists.org/lookup/suppl/doi:10.1242/jcs.121129/-/DC1

References

Ananthakrishnan, R. and Ehrlicher, A. (2007). The forces behind cell movement. *Int. J. Biol. Sci.* **3**, 303-317.

Berridge, M. J., Bootman, M. D. and Roderick, H. L. (2003). Calcium signalling: dynamics, homeostasis and remodelling. *Nat. Rev. Mol. Cell Biol.* **4**, 517-529.

Chen, Y. F., Chiu, W. T., Chen, Y. T., Lin, P. Y., Huang, H. J., Chou, C. Y., Chang, H. C., Tang, M. J. and Shen, M. R. (2011). Calcium store sensor stromal-interaction molecule 1-dependent signaling plays an important role in cervical cancer growth, migration, and angiogenesis. *Proc. Natl. Acad. Sci. USA* **108**, 15225-15230.

Chiu, W. T., Tang, M. J., Jao, H. C. and Shen, M. R. (2008). Soft substrate up-regulates the interaction of STIM1 with store-operated Ca^{2+} channels that lead to normal epithelial cell apoptosis. *Mol. Biol. Cell* **19**, 2220-2230.

Feske, S. (2009). ORAI1 and STIM1 deficiency in human and mice: roles of store-operated Ca2+ entry in the immune system and beyond. *Immunol. Rev.* **231**, 189-209.

Fu, J., Wang, Y. K., Yang, M. T., Desai, R. A., Yu, X., Liu, Z. and Chen, C. S. (2010). Mechanical regulation of cell function with geometrically modulated elastomeric substrates. *Nat. Methods* **7**, 733-736.

Kadir, S., Astin, J. W., Tahtamouni, L., Martin, P. and Nobes, C. D. (2011). Microtubule remodelling is required for the front-rear polarity switch during contact inhibition of locomotion. *J. Cell Sci.* **124**, 2642-2653.

Kanchanawong, P., Shtengel, G., Pasapera, A. M., Ramko, E. B., Davidson, M. W., Hess, H. F. and Waterman, C. M. (2010). Nanoscale architecture of integrin-based cell adhesions. *Nature* **468**, 580-584.

Lawson, C., Lim, S. T., Uryu, S., Chen, X. L., Calderwood, D. A. and Schlaepfer, D. D. (2012). FAK promotes recruitment of talin to nascent adhesions to control cell motility. *J. Cell Biol.* **196**, 223-232.

Middelbeek, J., Kuipers, A. J., Henneman, L., Visser, D., Eidhof, I., van Horssen, R., Wieringa, B., Canisius, S. V., Zwart, W., Wessels, L. F. et al. (2012). TRPM7 is required for breast tumor cell metastasis. *Cancer Res.* **72**, 4250-4261.

Mierke, C. T., Rösel, D., Fabry, B. and Brábek, J. (2008). Contractile forces in tumor cell migration. *Eur. J. Cell Biol.* **87**, 669-676.

Milner, R. and Campbell, I. L. (2002). Cytokines regulate microglial adhesion to laminin and astrocyte extracellular matrix via protein kinase C-dependent activation of the alpha6beta1 integrin. *J. Neurosci.* **22**, 1562-1572.

Monet, M., Lehen'kyi, V., Gackiere, F., Firlej, V., Vandenberghe, M., Roudbaraki, M., Gkika, D., Pourtier, A., Bidaux, G., Slomianny, C. et al. (2010). Role of cationic channel TRPV2 in promoting prostate cancer migration and progression to androgen resistance. *Cancer Res.* **70**, 1225-1235.

Monteith, G. R., Davis, F. M. and Roberts-Thomson, S. J. (2012). Calcium channels and pumps in cancer: changes and consequences. *J. Biol. Chem.* **287**, 31666-31673.

Oh-hora, M., Yamashita, M., Hogan, P. G., Sharma, S., Lamperti, E., Chung, W., Prakriya, M., Feske, S. and Rao, A. (2008). Dual functions for the endoplasmic reticulum calcium sensors STIM1 and STIM2 in T cell activation and tolerance. *Nat. Immunol.* **9**, 432-443.

Parekh, A. B. (2010). Store-operated CRAC channels: function in health and disease. *Nat. Rev. Drug Discov.* **9**, 399-410.

Prevarskaya, N., Skryma, R. and Shuba, Y. (2011). Calcium in tumour metastasis: new roles for known actors. *Nat. Rev. Cancer* **11**, 609-618.

Putney, J. W., Jr (2005). Capacitative calcium entry: sensing the calcium stores. *J. Cell Biol.* **169**, 381-382.

Qu, B., Al-Ansary, D., Kummerow, C., Hoth, M. and Schwarz, E. C. (2011). ORAI-mediated calcium influx in T cell proliferation, apoptosis and tolerance. *Cell Calcium* **50**, 261-269.

Ridley, A. J. (2011). Life at the leading edge. *Cell* **145**, 1012-1022.

Sanz-Moreno, V., Gaggioli, C., Yeo, M., Albrengues, J., Wallberg, F., Viros, A., Hooper, S., Mitter, R., Féral, C. C., Cook, M. et al. (2011). ROCK and JAK1 signaling cooperate to control actomyosin contractility in tumor cells and stroma. *Cancer Cell* **20**, 229-245.

Tan, J. L., Tien, J., Pirone, D. M., Gray, D. S., Bhadriraju, K. and Chen, C. S. (2003). Cells lying on a bed of microneedles: an approach to isolate mechanical force. *Proc. Natl. Acad. Sci. USA* **100**, 1484-1489.

Várnai, P., Hunyady, L. and Balla, T. (2009). STIM and Orai: the long-awaited constituents of store-operated calcium entry. *Trends Pharmacol. Sci.* **30**, 118-128.

Vicente-Manzanares, M., Ma, X., Adelstein, R. S. and Horwitz, A. R. (2009). Non-muscle myosin II takes centre stage in cell adhesion and migration. *Nat. Rev. Mol. Cell Biol.* **10**, 778-790.

Wei, C., Wang, X., Chen, M., Ouyang, K., Song, L. S. and Cheng, H. (2009). Calcium flickers steer cell migration. *Nature* **457**, 901-905.

Xu, P., Lu, J., Li, Z., Yu, X., Chen, L. and Xu, T. (2006). Aggregation of STIM1 underneath the plasma membrane induces clustering of Orai1. *Biochem. Biophys. Res. Commun.* **350**, 969-976.

Yang, S., Zhang, J. J. and Huang, X. Y. (2009). Orai1 and STIM1 are critical for breast tumor cell migration and metastasis. *Cancer Cell* **15**, 124-134.

Yilmaz, M. and Christofori, G. (2009). EMT, the cytoskeleton, and cancer cell invasion. *Cancer Metastasis Rev.* **28**, 15-33.